

**VULNERABILITY ASSESSMENT OF CAR NICOBAR TO TSUNAMI HAZARD  
USING NUMERICAL MODEL**

**Tune Usha<sup>1</sup>, M V Ramana Murthy<sup>1</sup>, N T Reddy<sup>1</sup>, T S Murty<sup>2</sup>**

ICMAM-PD, Ministry of Earth Sciences, Govt. of India, NIOT Campus, Pallikaranai, Chennai  
600 100., Fax : 044-22460657, Phone : 044-22460991, email : usha@icmam.gov.in

\* - University of Ottawa, Ottawa, Canada, Phone : +1-6137395445, Fax : +1-613 562 5173  
e-mail:smurty@hotmail.com

**ABSTRACT**

The December 26, 2004 Sumatra earthquake's epicenter was 163 kms away from Great Nicobar, the southern most island from the archipelago and hence it was strongly felt in the entire Andaman & Nicobar group of islands including Car Nicobar. 3400 people have lost their lives and most of the vital infrastructure were completely destroyed. The presents study aims to understand the vulnerability of the Car Nicobar coast to tsunami hazard from varied sources by using numerical model of tsunami propagation and run-up and compare it with the field data on inundation collected immediately after the tsunami using real time kinematic GPS. A tsunami vulnerability database has been builtup by modelling the past earth quakes recorded in this region. Elevation data collected using Airborne Laser Terrain Mapper (ALTM) was used to generate the inundation scenarios. A GIS database on the tsunami vulnerability of Car Nicobar to tsunami hazard is generated which would be immense use in mitigation and planning.

## **1.0 INTRODUCTION**

The idyllic island of Car Nicobar, which bore the full fury of the tsunami in December 2004, lies in the heart of the Andaman and Nicobar islands archipelago in the Indian Ocean. It is the northernmost of the Nicobar Islands, which in turn are the southern part of the Indian Union territory of the Andaman and Nicobar islands. It lies at 9°10'N 92°45'E and has an area of 127 km<sup>2</sup> and is a very small Island, in comparison to the Middle Andaman or South Andaman. The climate of Car Nicobar Island is tropical, as it is just 9 degree from the equator, with an annual rainfall of 400 mm.

The 26th December, 2004 earthquake was followed by high tsunami tidal waves which caused extensive damages in parts of Andaman and Nicobar such as Port Blair harbour, Jetties at Aberdeen, Phoenix Bay, Junglighat and Haddo which were flooded by high tidal waters. However, the extent of damage, loss of life and property in Car Nicobar was unprecedented due to the combined action of high waves and subsidence of land to an extent of 1.3m due to the earthquake. The side of the islands facing the epicenter was the most vulnerable. The Nicobarese villages of Malacca and Kakana on the southeastern side of the island suffered heavy casualties while on the northeastern side, people in the villages of Sawai, Arong, Teatop moved deeper into the forest and formed new settlements. The Malacca jetty was totally destroyed.

## **2.0 TSUNAMI VULNERABILITY OF THE ANDAMAN AND NICOBAR ISLANDS**

India's vulnerability to tsunami-caused destruction was estimated as very low, if not non-existent until the 2004 tsunami event. As a result, not only was there no effort to set up an advance warning and international networking system, but tsunami-vulnerability was not one of the factors taken into account in the determination of the location of our nuclear and space launching establishments and in designing their safety features. Similarly, this vulnerability was not taken into consideration while determining the location of our military establishments in the Andaman and Nicobar Islands and their safety features. However, Andaman and Nicobar islands have not been totally immune to tsunamis, because at least five historical earthquakes have been known to have triggered a tsunami that hit the islands of Andaman and Nicobar (Fig.1).

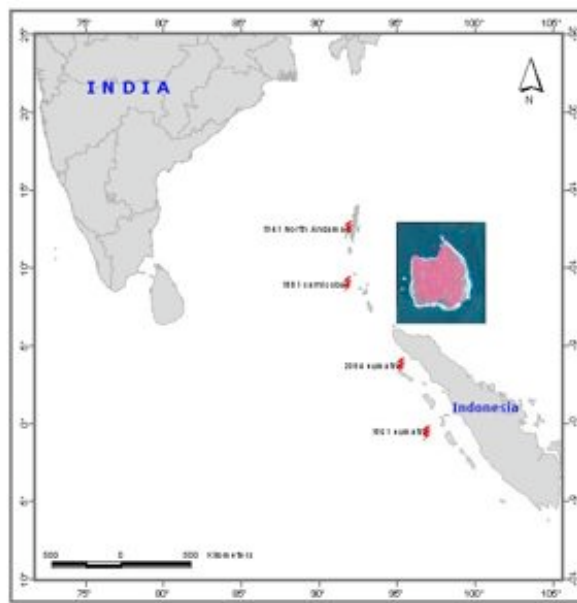


Fig. 1. Tsunamigenic sources that threaten Car Nicobar

### 2.1 Car Nicobar, India, 1847

The first of the three large historical earthquakes in the Andaman/Nicobar region for which information is available occurred on 31<sup>st</sup>, October, 1847, however no original account of the 1847 earthquake survived.

### 2.2 Car Nicobar, India, 1881

The second recorded earthquake was on 31<sup>st</sup> December 1881 at Car Nicobar. Data for the study of this earthquake were compiled by Oldham (1884) who, on the basis of astronomical clock recordings in Madras (Chennai) and Calcutta (Kolkatta), believed the earthquake occurred on the locus of these two cities beneath the Bay of Bengal (400 km west of the Andaman Islands). Seismographs had yet to be invented but tide gauges at eight harbors surrounding the Bay of Bengal recorded the largest surface waves and the resulting tsunami, and these data provide a powerful constraint on timing and rupture parameters. The earthquake with magnitude  $M_w$ -7.9 is calculated to have occurred near and west of Car Nicobar with two reverse slip ruptures.

### 2.3 Andaman, India, 1941

The most recent of the major earthquakes in the Andaman islands preceding the recent rupture of 2004 occurred in 1941, a year before Japanese occupation of the islands. However, the earthquake was described only after the Second World War [Krishnan, 1953; Jhingran, 1953] Although the tsunami generated by the 1941 earthquake is stated to have caused much loss of life

along the east coast of India [Murty and Rafiq, 1991] no official (or unofficial) account of the impact of the remote tsunami has been discovered. Jhingran describes the loss of low-lying western-facing forest cover on the Andamans, presumably by a tsunami but mentions no loss of life. Eyewitness reports published informally by the Society of Andaman and Nicobar Ecology (SANE) following the 2004 earthquake add further details to the official 1941 accounts. The central watch-tower of the cellular jail in Port Blair collapsed along with a hospital and other masonry structures. Eyewitnesses speak of subsidence of Ross Island (as in the recent earthquake), requiring its abandonment in favor of the current mainland capital, Port Blair.

#### **2.4 Sumatra, Indonesia, 2004**

The worst tsunami disaster in living history was caused by an earthquake in the Indian Ocean off the island of Sumatra measuring 9.3Mw. More than 300 000 people were killed in eight Asiatic countries (in particular Indonesia/Sumatra, Sri Lanka, India, Thailand, Myanmar, Maldives, Malaysia and Bangladesh). The flood wave even reached coastlines several thousand kilometres away, like East and Southeast Africa. There were also casualties in Somalia, Tanzania, Kenya, Madagascar and the Seychelles.

#### **2.5 Sumatra , Indonesia, 1861**

Based on past historical records and the tsunami of the recent past, an attempt has been made to study the vulnerability of the islands of Andaman and Nicobar to tsunamis. Car Nicobar by virtue of its proximity to the earthquake source and low land elevation was severely damaged and hence was extensively surveyed for extent of inundation and runup immediately after the tsunami. The field data collected was used to validate the numerical models used to calculate the vulnerability of the island due to tsunami hazard. the A GIS based risk atlas is developed using Numerical models to study the extent of inundation and run-up for various historic earthquake scenarios. Inundation scenarios have been generated for four past earthquake scenarios. In order to assess the maximum extent of inundation and run-up that could occur in future, a hypothetical earthquake scenario was also generated by loading the Sumatra 2004 earthquake seismic parameters on the Car Nicobar source.

### 3.0 METHODOLOGY

The main objective of this work is to provide an estimate of wave height and extent of inundation in the event of a tsunami. Given the time constraints of computing the three stages of tsunami modeling, namely, wave generation, propagation and inundation in real time, the work is expedited by generating a database of pre-computed scenarios, which is found to be an useful tool in tsunami mitigation. The pre-computed database contains information about tsunami propagation in the open ocean from a multitude of potential sources. When a tsunami event occurs, an initial source is selected from the pre-computed database. In the initial stages of the tsunami, this selection is based only on the available seismic information for the earthquake event, similar to one of the pre-computed scenario. For the identified earthquake scenario, the large scale inundation map is selected from the database.

Inundation studies can be conducted taking a probabilistic approach in which multiple tsunami scenarios are considered, and an assessment of the vulnerability of the coast to tsunami hazard is evaluated, or they may focus on the effect of a particular ‘worst case scenario’ and assess the impact of such a particularly high impact event on the areas under investigation. The results of a tsunami inundation study should include information about the maximum wave height and maximum inundation line. This information can be used by emergency managers and urban planners primarily to establish evacuation routes and location of vital infrastructure. On the basis of the model prediction, vulnerability maps will be prepared which will be useful in disaster management and mitigation activities. These maps help in defining the limits of construction of new essential facilities and special occupancy structures in tsunami flooding zones

An inundation modeling study attempts to recreate the tsunami generation in deep waters, wave propagation to the impact zone and inundation along the study area. To reproduce the correct wave dynamics during the inundation computations high resolution bathymetric and topographic grids are required. The high quality bathymetric and topographic data sets needed for development of inundation maps require maintenance and upgrades as better data becomes available and coastal changes occur. In the present study elevation datasets have been collected using Airborne Laser Terrain Mapper (ALTM) for a distance of 2km from the coast all around the island. ALTM datasets were corrected for the mean sea level and the vertical error was found to be about 0.35m. For higher altitudes inland, 1:25000 toposheet was used to derive the elevation data. On the sea side, bathymetry data was obtained from C-Map and NHO charts. The General

bathymetric chart of the oceans (GEBCO) was used to populate the deep sea regions. The datasets were so built so as to have very precise data for the near coastal regions both on the land and sea side which plays the dominant part for inundation studies and the offshore datasets were populated using global bathymetry datasets (Fig.2).

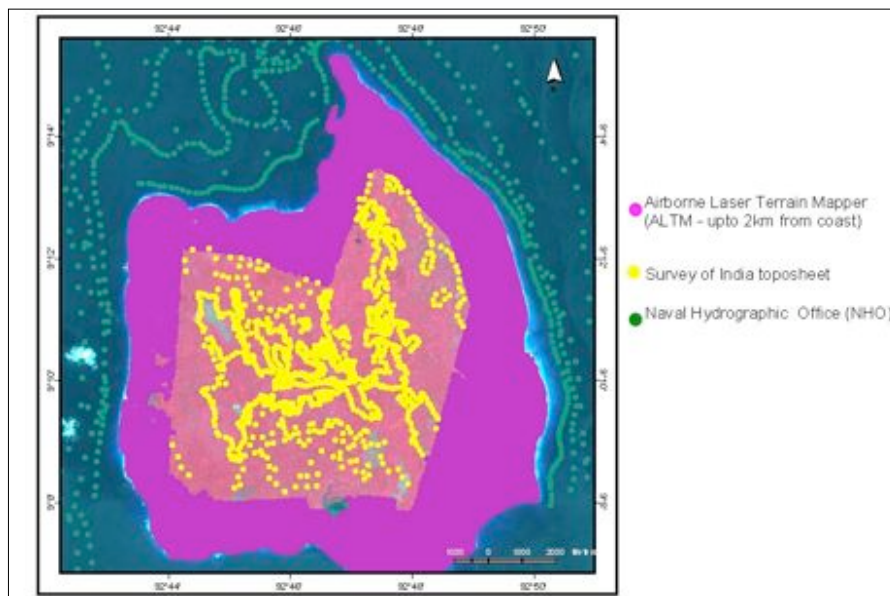


Fig 2. Data used to populate the near coastal regions

#### 4.0 NUMERICAL MODEL FOR TSUNAMI INUNDATION

The use of numerical modeling to determine the potential run-ups and inundation from a local or distant Tsunami is recognized as useful and important tool, since data from past tsunamis are usually insufficient to plan future disaster mitigation and management plans. Sufficiently accurate modeling techniques have been developed in the recent years, and these models require proper inputs on detailed bathymetry and topographic data for the area being modeled. In the present study a finite difference code of TUNAMI N2 (Imamura, 1996) was employed to predict the inundation. The parameters used for computation of the sea surface deformation at source for various historical earthquakes are given in Table 1.

Table 1. Parameters used for computation of sea surface deformation at source

Parameters	2004 Sumatra	1941 Andaman	1881 Car Nicobar	1861 Sumatra	Worst-case
Source	Sumatra	North Andaman	Car Nicobar	Sumatra	Car Nicobar
Longitude	95.85 <sup>0</sup> E	92.5 <sup>0</sup> E	92.43 <sup>0</sup>	97.5 <sup>0</sup>	92.43 <sup>0</sup>
Latitude	3.32 <sup>0</sup> N	12.1 <sup>0</sup> N	8.52 <sup>0</sup>	-1.00	8.52 <sup>0</sup>
Magnitude	9.3 Mw	7.7 Mw	7.9 Mw	8.5 Mw	9.3 Mw
Slip	15 m	5 m	5 m	4 m	15 m
Fault Length	500 km	200 km	200 km	305 Km	500 km
Fault Width	150 km	80 km	80 km	101 Km	150 km
Strike Angle	345 <sup>0</sup>	20 <sup>0</sup>	350 <sup>0</sup>	320 <sup>0</sup>	345 <sup>0</sup>
Dip Angle	15 <sup>0</sup>	20 <sup>0</sup>	25 <sup>0</sup>	12 <sup>0</sup>	15 <sup>0</sup>
Rake Angle	90 <sup>0</sup>	90 <sup>0</sup>	90 <sup>0</sup>	90 <sup>0</sup>	90 <sup>0</sup>
Focal Depth	20 km	30 km	15 km	30 km	20 km

These seismic parameters are provided as input to construct dislocation for determination of the static Tsunami source (initial wave) in the domain. The predictions of the models are directly related to the quality of the data used to create the bathymetry and topography of the model area. Considerable time, resource and effort are necessary to collect high resolution bathymetry and elevation data of the coastal areas. The model results obtained using the high resolution bathymetry and elevation data are calibrated and validated using field observations. The model once validated can be used for creating different scenarios of extreme inundation and run-up by varying the source parameters that actually trigger the tsunami.

#### 4.1 Generation of computational grids

To create the computational grids for tsunami model, ALTM data and 1:25000 Survey of India toposheet and NHO charts was used along with GEBCO and SRTM datasets. As a nested grid system was used to run the model, the inner most study area grid was constructed using highly accurate altm dataset and NHO chart values.

## 4.2 Field measurements

Immediately after the tsunami, field measurements on inundation and runup were made along the Car Nicobar coast specially along the Indian Airforce Base at Malacca. Run-up measurements at different sites along the coasts were made using Realtime Kinematic Global Positioning System (RTKGPS). In Car Nicobar a maximum runup of about 7m and an inundation of 1km was observed near Malaca (Table 2).

Table 2. Field Measurements at Car Nicobar on Inundation and Run-up

Id	Latitude	Longitude	Elevation (m)	Inundation (m)
1	9.173491884	92.82259519	2.4813	695
2	9.157835800	92.82230271	8.0579	900
3	9.161034506	92.82278315	8.3134	893
4	9.164605948	92.82333409	7.1946	870
5	9.164617939	92.82330192	7.2213	874
6	9.164629949	92.82326922	7.1634	876
7	9.164664574	92.82317327	7.0282	880
8	9.164688440	92.82310983	6.9155	876
9	9.164699524	92.82307782	6.8499	895
10	9.164722952	92.82301324	6.7947	882
11	9.164735309	92.82298218	6.7301	910
12	9.165120533	92.82363841	6.6481	842
13	9.166610636	92.82404471	5.8565	790

## 4.3 Validation of model results

The model results were validated using the field data on inundation collected immediately after the tsunami (Table 3, Fig.3 and Fig.4).

Table 3. Observed and Predicted Inundation for 2004 Sumatra earthquake source

Id	Latitude	Longitude	Observed (m)	Predicted (m)
1	9.173491884	92.82259519	695	700
2	9.157835800	92.82230271	876	600
3	9.161034506	92.82278315	893	870
4	9.164605948	92.82333409	870	880
5	9.164617939	92.82330192	874	850
6	9.164629949	92.82326922	876	950
7	9.164664574	92.82317327	880	947
8	9.164688440	92.82310983	876	945
9	9.164699524	92.82307782	895	950
10	9.164722952	92.82301324	882	980

11	9.164735309	92.82298218	910	990
12	9.165120533	92.82363841	842	844
13	9.166610636	92.82404471	790	789

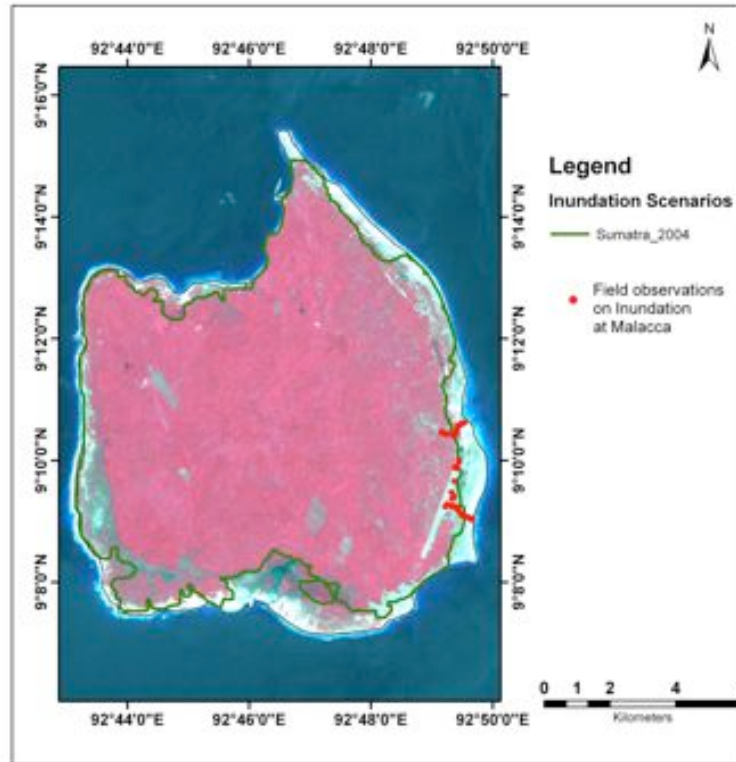


Fig. 3. Validation of model results using field data

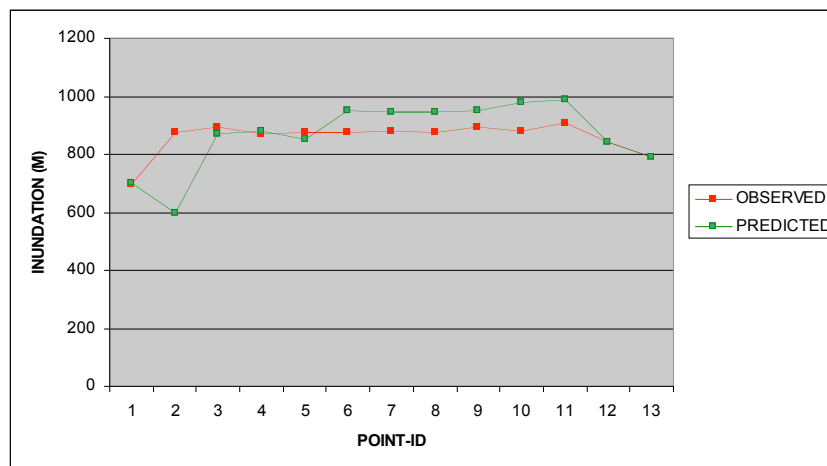


Fig. 4. Comparison between observed and predicted inundation

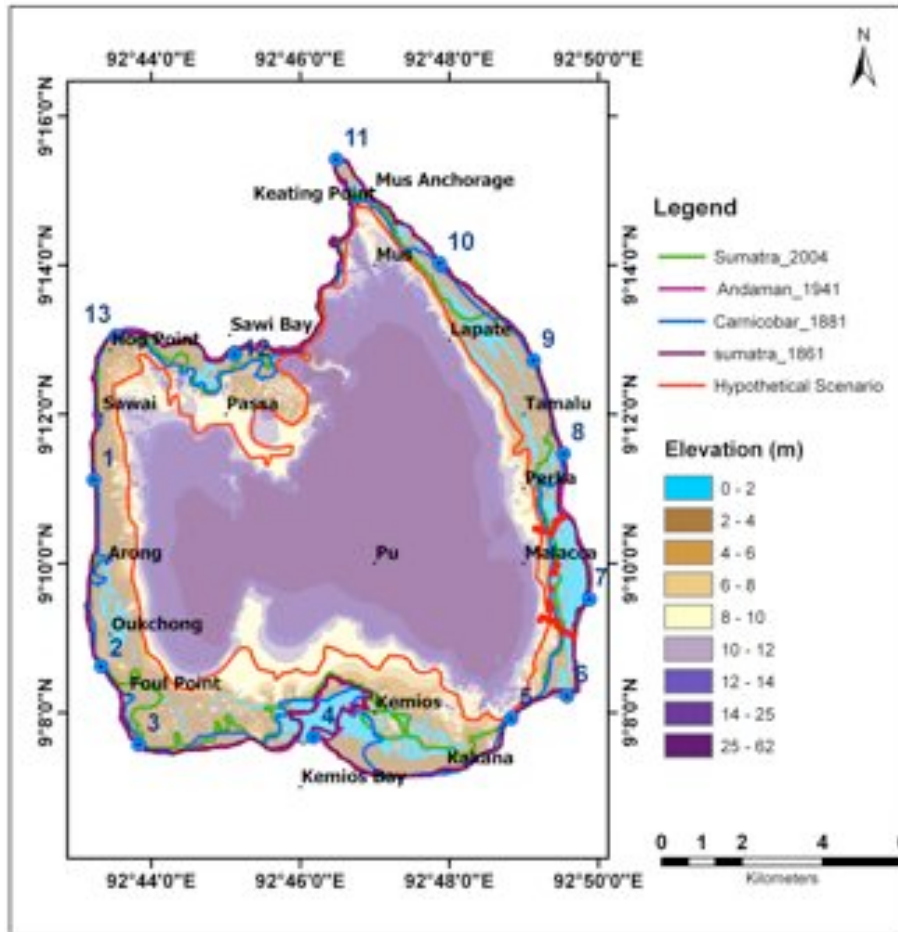


Fig. 5. Extent of Inundation for Various earthquake scenarios

## 5.0 OBSERVATIONS AND DISCUSSION

The extent of inundation due to four historical earth quakes and one hypothetical worst case scenario is given in Fig.5. The inundation and runup predicted along the selected points along the shore are tabulated below (Table 4 and 5).

Table 4. Predicted Inundation at Car Nicobar due to the various Tsunamigenic sources

Inundation in meters.

Id	Longitude	Latitude	Sumatra 2004	Car Nicobar 1881	Andaman 1941	Sumatra 1861	Hypothetical Scenario
1	92.720520	9.185373	120	-	-	-	921
2	92.722187	9.143707	106	-	-	-	1290
3	92.730520	9.126207	340	141	-	-	1886
4	92.769687	9.127873	1630	971	1557	1570	2302
5	92.813853	9.132040	82	66	-	-	130
6	92.826353	9.137040	768	727	160	157	1215
7	92.831353	9.158707	808	940	110	141	1386
8	92.825520	9.191207	388	97	-	-	1205
9	92.818853	9.212040	117	-	-	-	1413
10	92.798020	9.234540	526	102	-	-	643
11	92.774687	9.257040	1183	1267	-	-	1375
12	92.752050	9.215474	532	607	138	184	2896
13	92.725520	9.218707	121	133	-	-	1231

Table 5. Predicted Run-up at Car Nicobar due to the various Tsunamigenic sources

Runup in meters.

Id	Longitude	Latitude	Sumatra 2004	Car Nicobar 1881	Andaman 1941	Sumatra 1861	Hypothetical Scenario
1	92.72052	9.185373	2.34	2.65	0.24	0.36	6.96
2	92.72219	9.143707	2.75	2.75	0.28	0.58	6.60
3	92.73052	9.126207	2.66	2.40	0.31	0.59	7.69
4	92.76969	9.127873	3.44	3.68	0.64	1.02	8.49
5	92.81385	9.13204	5.14	3.63	0.81	1.08	7.34
6	92.82635	9.13704	3.77	3.31	0.33	0.71	5.26
7	92.83135	9.158707	2.07	3.48	0.18	0.49	6.10
8	92.82552	9.191207	1.97	2.50	0.14	0.37	5.04
9	92.81885	9.21204	2.06	2.81	0.13	0.32	5.31
10	92.79802	9.23454	3.67	2.67	0.20	0.40	4.48
11	92.77469	9.25704	2.59	2.24	0.27	0.41	3.41
12	92.75205	9.215474	2.92	3.53	0.44	0.65	10.40
13	92.72552	9.218707	1.75	2.10	0.23	0.50	5.61

### 5.1 Inundation and run-up due to Sumatra, Indonesia, December 26, 2004 earthquake

Inundation and Water level at Car Nicobar due 2004 Sumatra Tsunami caused by an earthquake of 9.3 Mw and at a distance of 750km, SE of Car Nicobar is shown in Fig. 6. The maximum inundation at the coast from the shore was 720m in Malaca (Point 6) whereas the water entered further inland through creeks (Pt.4 and Pt.11). The maximum run-up was 5.1m. Along the coast there are significant spatial gradients in tsunami run up signatures, which are attributed to topographic profiles along the coastline. The tsunami surge penetrates along the shore up to berm level along straight coast and penetrated inland large distances inland wherever low lands/ creeks connected to sea. Along the coast the run up heights varied between 2.0m to 5.1 m and the run up distances from 100 to 800m.

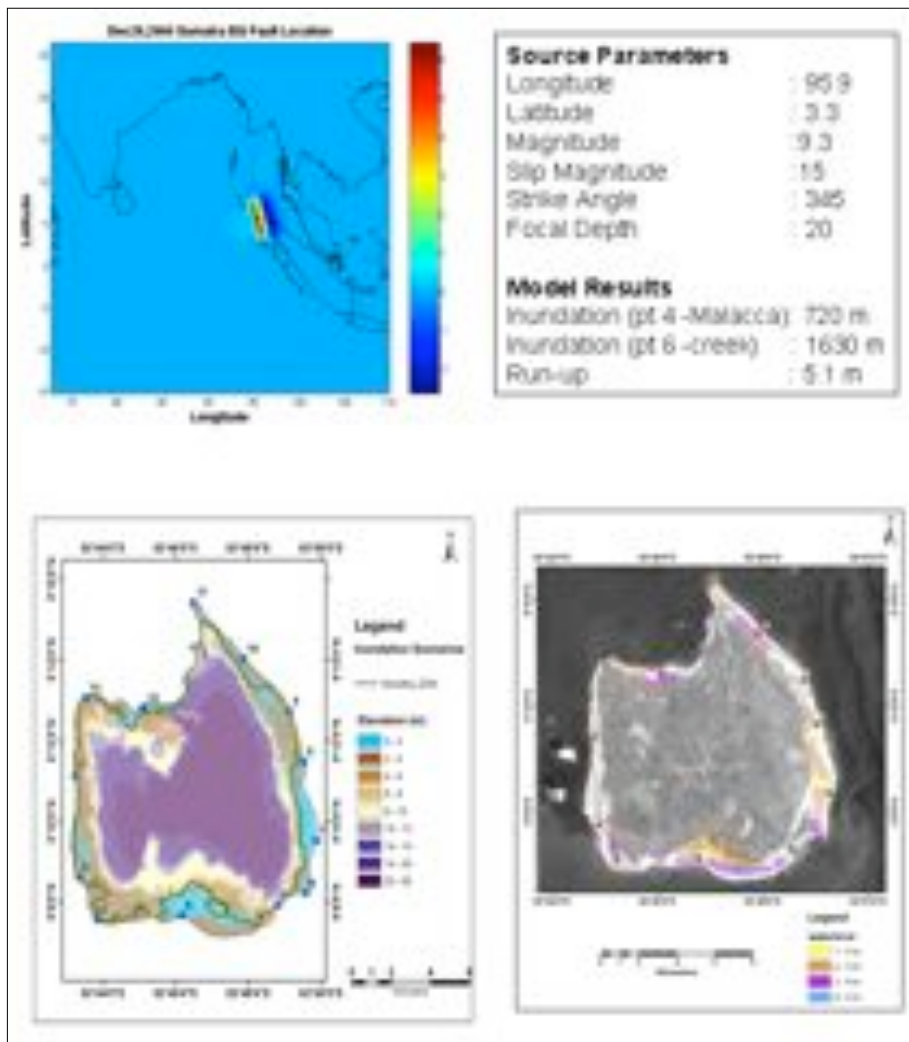


Fig.6 Inundation and Water level at Car Nicobar for 2004 Sumatra Tsunami – Earth quake of 9.3 Mw and at a distance of 750km, SE of Car Nicobar

## 5.2 Inundation and run-up due to Car Nicobar, India, December 31, 1881 earthquake

Inundation and Water level at Car Nicobar due 1881 Car Nicobar Tsunami caused by an earth quake of 7.9 Mw and at a distance of 75km, SW of Car Nicobar is shown in Fig.7. The maximum inundation at the coast from the shore was 900m (Point 7) whereas, the water entered further inland through creeks (Pt.4 and Pt.11). The maximum run-up was 3.5m. Along the coast the run up heights varied between 2.0m to 3.5 m and the run up distances from 100 to 900m.

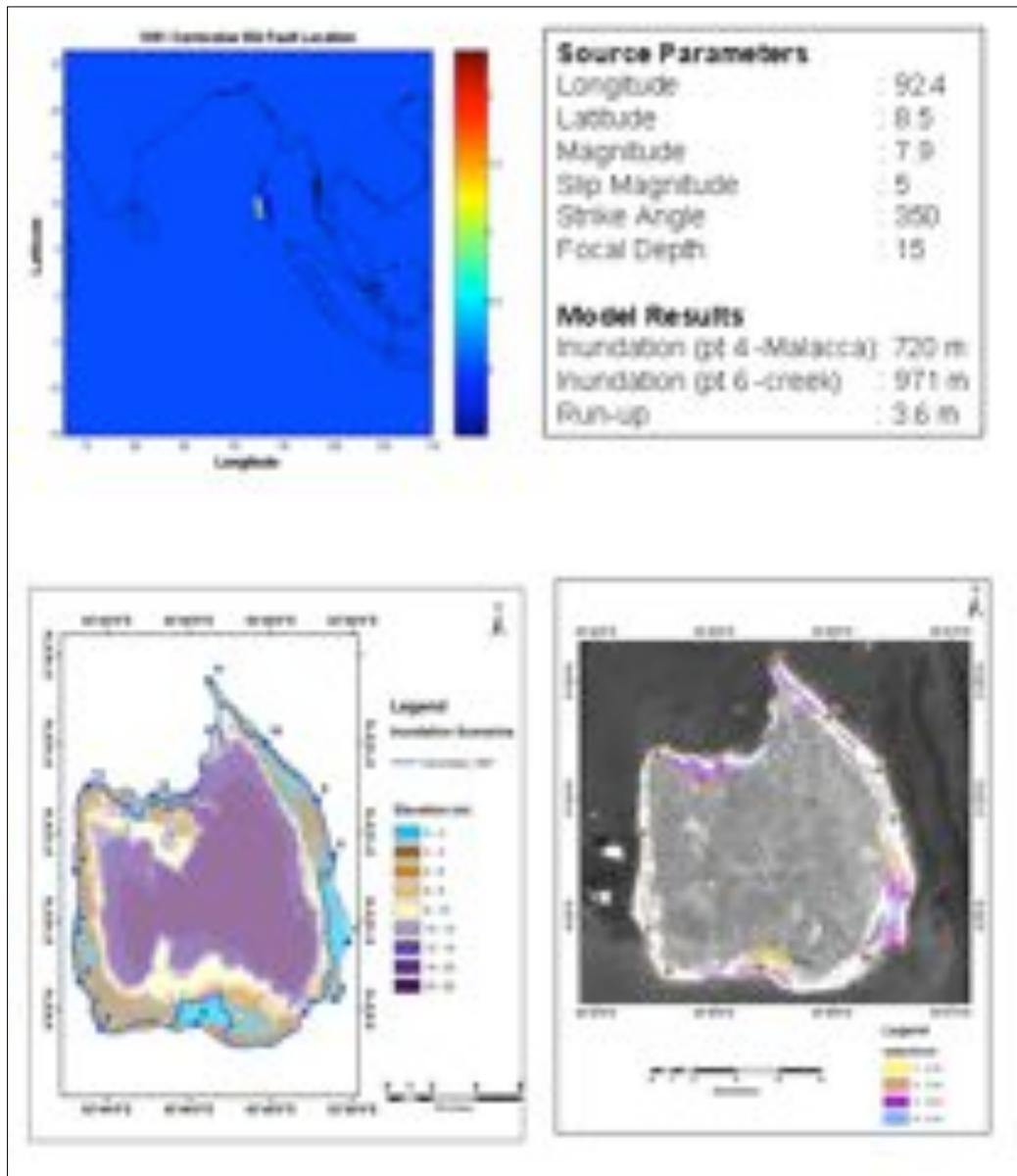


Fig.7. Inundation and Water level at Car Nicobar for 1881 Car Nicobar Tsunami – Earth quake of 7.9 Mw and at a distance of 75km, SW of Car Nicobar

### 5.3 Inundation and run-up due to Andaman 26 June 1941 earthquake

Inundation and Water level at Car Nicobar due 1941 Andaman tsunami caused by an earth quake of 7.7 Mw and at a distance of 330km, North of Car Nicobar is shown in Fig.8. Though there was an observed rise in water level it was very minimal and the inundation inland was also not very significant. However water entered inland through creeks upto a distance of 1.5km.

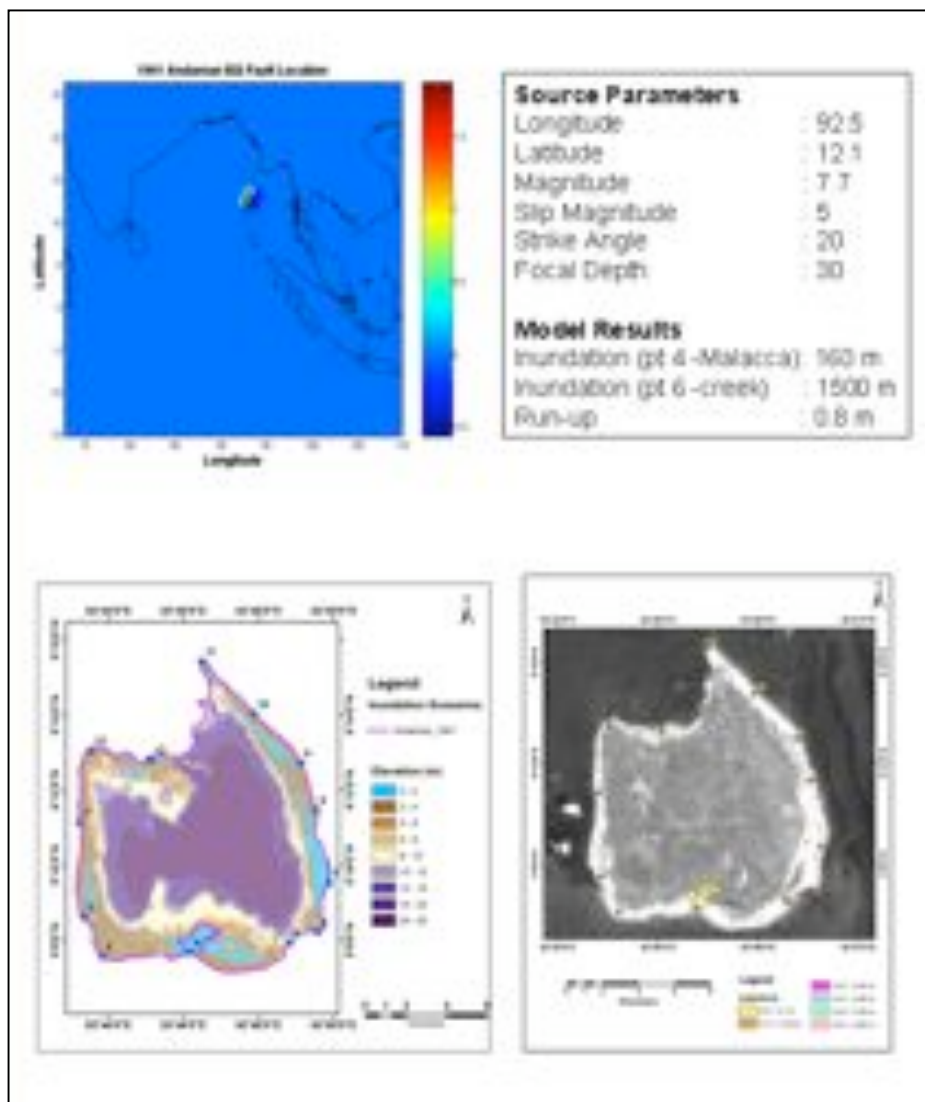


Fig.8. Inundation and Water level at Car Nicobar for 1941 Andaman Tsunami – Earth quake of 7.7 Mw and at a distance of 330km, North of Car Nicobar

### 5.4 Inundation and run-up due to Sumatra 1861 earthquake

Inundation and Water level at Car Nicobar due 1861 Sumatra tsunami caused by an earthquake of 8.5 Mw and at a distance of 810km, NE of Car Nicobar is shown in Fig. 9. Though there was an observed rise in water level it was very minimal and the inundation inland was also not very significant. However water entered inland through creeks upto a distance of 1.5km.

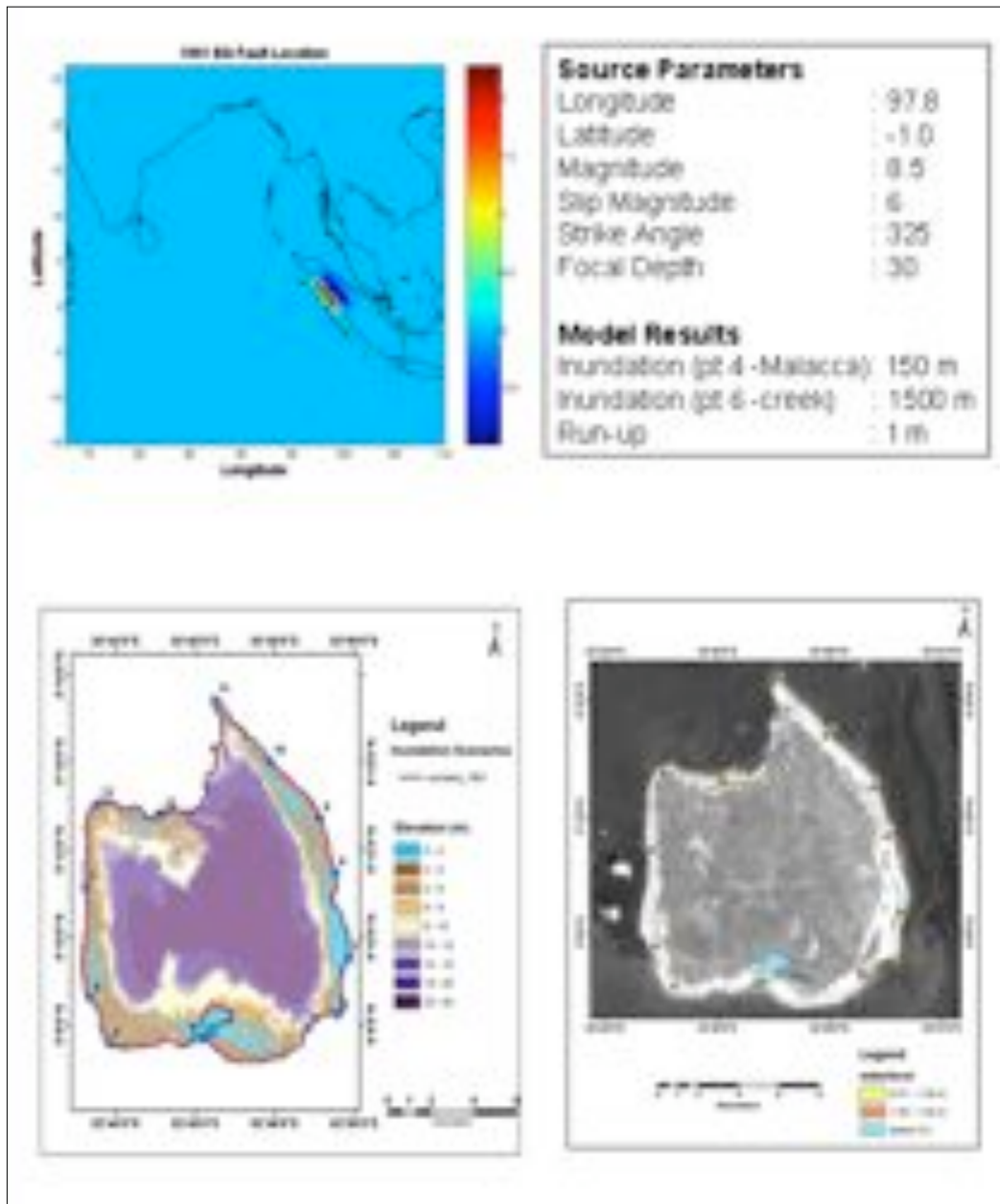


Fig. 9 Inundation and Water level at Car Nicobar for 1861 Sumatra Tsunami – Earth quake of 8.5 Mw and at a distance of 810 km, NE of Car Nicobar

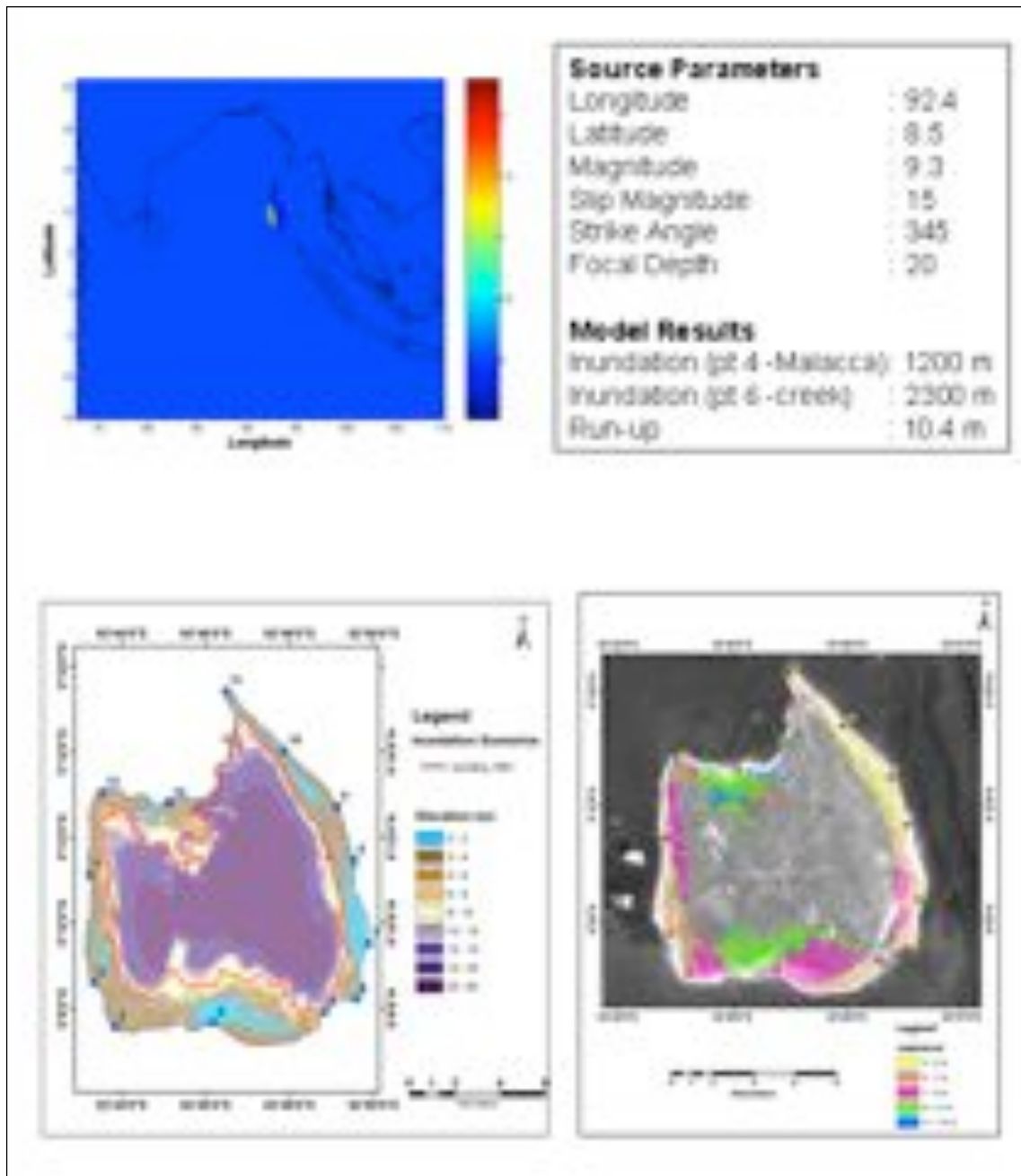


Fig. 10 Inundation and Water level at Car Nicobar for worst case scenario Tsunami – Earth quake of 9.3 Mw and at a distance of 75 km, SW of Car Nicobar

## 5.5 Inundation and run-up due to a hypothetical worst case scenario

A worst case scenario was developed by forcing the Sumatra 2004 earth parameters on the 1881 Car Nicobar earthquake location. Since this location was only at a distance of 75km SW of Car Nicobar large scale inundation and run-up heights were predicted by the model. The maximum inundation was about 3km (point 12) while the maximum run-up as 10.40 m. The maximum inundation and run-up at Car Nicobar for historical earthquake scenarios and one hypothetical worst case scenario is listed below (Table 6).

Table 6 . Maximum inundation and run-up calculated along Car Nicobar coast

Location	Source Distance	Magnitude	Land inundation	Inundation-creeks	Max.up Runup
Sumatra-2004	750	9.3	720	1630	5.1
Andaman-1941	330	7.7	160	1597	0.8
Car Nicobar 1881	75	7.9	720	971	3.6
Sumatra-1861	810		150	1570	1
Worstcase scenario	75	9.3	1200	2300	10.4

## 6.0 HIGH WATER LEVELS

High Water Levels of Tsunami Persisted for Several days in A & N Islands and Media reports as well as scientific observations suggested that, even though the 26 December 2004 tsunami lasted only a few hours in A & N Islands, high waters persisted for several days. The results of the numerical model for 2004 Sumatra tsunami also indicate high water levels along the Car Nicobar coast. The question then is what physical processes is responsible for these high water levels. A brief explanation is provided below in terms of the so called Oscillations of the First Class (OFC) and Oscillations of the Second Class (OSC) in the oceans. The OFC are essentially gravity modes while the OSC are called rotational modes or elastoidal-elastoid inertia oscillations. The OFC would exist with or without earth's rotation but their frequency is modified due to earth's rotation, whereas the OSC owe their existence to earth's rotation.

The frequency range of OFC and OSC is separated by the so called pendulum day defined below;

$$2T_p = \frac{2\pi}{\omega \cdot \sin \theta}$$

$T_p$  = period of revolution of a Foucault Pendulum;  
 $\theta$  = latitude;  $\omega$  = angular velocity of earth's rotation  
 $\omega$  = Angular velocity of Earth's rotation

As can be seen from the above equation, the pendulum day, which is defined as the time taken by a Foucault Pendulum to complete one rotation, depends on the latitude. It is generally understood that once the long gravity wave energy from a tsunami (or a storm surge) gets trapped on the shelf around an island system, it will take at least one pendulum day (in reality it takes several pendulum days) for the energy to be gradually dissipated.

The pendulum day is estimated below for the southern extreme of the Nicobar Islands and northern extreme of the Andaman Islands.

Southern extreme =  $6^\circ$  N latitude

Length of pendulum day = 231 hours

Northern extreme =  $14^\circ$  N latitude

Length of pendulum day = 100 hours

The Andaman and Nicobar islands stretch from 6 degrees to 14 degrees North and pendulum days varies from 231 to 100 hours. Car Nicobar lies at 9 degree latitude and thus, one can speculate that the water levels stayed high in the Car Nicobar island due to trapping of the tsunami energy on the shelf.

## 7.0 CONCLUSIONS

The vulnerability of the Car Nicobar coast to tsunami hazard was studied using numerical models. High accuracy elevation data collected using ALTM survey was an invaluable for the coastal inundation modelling carried out on Car Nicobar coast for various past earthquake scenarios. The island seems to be most vulnerable along the Eastern and the southern side compared to the western side. Moreover the persistence of high water level around the island for many days after the tsunami is due to the length of the pendulum day in the Andaman and Nicobar islands which varies from 231 to 100 hours.

## ACKNOWLEDGEMENTS

We thank Dr. B R. Subramanian, Adviser and Sci-G, Ministry of Earth Sciences, ICMAM-PD, Government of India for the guidance and support extended to us during the entire course of this work.

## REFERENCES

- Aida, I. (1977) Tsunamis accompanied by Land slides, *Kaiyo-Kagaku. Monthly Journal of Marine Sciences, Japan*, 9, 103-110.
- Ammon, J. Charles, and J. Chen (2005) Rupture Process of the 2004 Sumatra-Andaman Earthquake. *Science*, 308, 1133-1139.
- Bilham, R. (2005) A Flying Start, Then a Slow Slip. *Science*, 308, 1126-1127.
- Goto, C. and N. Shuto Effects of Large Obstacles on Tsunami Inundations. pp. 521-525. In K. Iida and T. Iwasaki (eds.) *Tsunamis: Their Science and Engineering*, Terra Scientific, Tokyo/Reidel, 1983.
- Houston, J.R. and H.L. Butler (1979) A numerical model for tsunami inundation, Final Report, US Army Corps of Engineers, Hydraulic Laboratory, Waterways Experiment Station, Vicksburg, MS, Technical Report. HL-79-2.
- Imamura, F. Review of Tsunami Simulation with a Finite-Difference Method. pp. 25-42. In H. Yeh, P. Liu, and C. Synolakis (eds.) *Long-Wave Runup Models*, World Scientific, Singapore, 1996.
- Ioualaen, M., Asavanant, J., Kaewbanjak, N., Grilli, S.T., Kirby, J.T., and Watts, P (2007) Modelling the 26 December 2004 Indian Ocean tsunami: Case study of impact in Thailand, *J. Geophys. Res.*, 112, C07024
- Iwan, D.W. *Earthquake Spectra*, The professional journal of the earthquake engineering research institute, UNESCO and EERI, Special issue III, UNESCO, France, 2006.
- Kajiura, K. (1963) The Leading Wave of a Tsunami, *Bulletin Earthquake Research Institute*, 41(3), 535-571.
- Mansinha, L. and D.E. Smylie (1971) The Displacement Fields of Inclined faults, *Bulletin on Seismological Society of America*, 61, 1400-1433.
- Okada, Y. (1985) Surface Deformation due to Shear and Tensile Faults in a Half-Space. *Bulletin of Seismological Society of America*, 75 (4), 1135-1154.

- Satake, K. Tsunamis. pp. 437-451. In W.K. Lee, H. Kanamori, P.C. Jennings, and C. Kisslinger (eds.) International Handbook of Earthquake and Engineering Seismology, 2002.
- Shuto, N. and C. Goto (1978) Numerical Simulation of Tsunami Run-up. Coastal Engineering in Japan, 21, 13-20.
- Shuto, N., C. Goto, and F. Imamura (1990) Numerical simulation as a means of warning for near field tsunamis. Journal of Coastal Engineering in Japan, 33(2), 173-193.
- Shuto, N (1991) Numerical Simulation of Tsunamis- Its Present and Near Future, Natural Hazards, 4, 171-191.
- Stein, S. and E. Okal (2005) Speed and size of Sumatra earthquake. Nature, 434, 581-582.
- Synolakis, C.E. Tsunami and Seiche. pp. 9.1-9.79. In W.F. Chen and C. Scawthorn (eds.) Earthquake Engineering Handbook, CRC Press, Washington D.C., 2004.
- Takeda, H. (1984) Numerical Simulation of Run-up by Variable Transformation. Oceanographical Journal of Japan, 40, 271-278.
- Titov, V. and F. Gonzalez (1997) Implementation and testing of the method of splitting tsunami (MOST) model, NOAA Technical Memorandum ERL PMEL-112.
- Titov, V.V. and C.E. Synolakis (1997) Extreme Inundation Flows during the Hokkaido-Nansei-Oki Tsunami. Geophysics Research Letter, 24 (11), 1315-1318.
- Uda, T. (1988) Numerical simulation and experiment on tsunami run-up. Coastal Engineering In Japan, 31, 87-104.